

A study of cortical bone microdamage and crack morphology utilising confocal microscopy and sequential labelling

J. Codrington^{1,2}, J. Kuliwaba^{2,3}, K. Zarrinkalam² and N. Fazzalari^{2,3}

¹ School of Mechanical Engineering, The University of Adelaide, Adelaide, SA 5005, Australia, email: john.codrington@adelaide.edu.au

² Bone and Joint Research Laboratory, SA Pathology, Adelaide, SA 5000, Australia, email: julia.kuliwaba@imsv.sa.gov.au, nick.fazzalari@imsv.sa.gov.au

³ Discipline of Pathology, The University of Adelaide, Adelaide, SA 5005, Australia

ABSTRACT. *The formation and accumulation of microdamage in bone plays an important role in the occurrence of stress and fragility fractures as well as in the initiation of bone remodelling. In this study a novel technique is presented for the investigation of bone microdamage and crack morphology using laser scanning confocal microscopy and sequential labelling with chelating fluorochromes. Compact tension fracture specimens machined from bovine tibial cortical bone, were mechanically tested in a wedge loaded crack-propagating tool. Sequential labelling with xylenol orange and calcein allowed for the crack propagation and microdamage progression to be assessed at each stage using confocal microscopy. Both two-dimensional confocal images and three-dimensional z-series reconstructions displayed the formation of a microdamage process zone and wake surrounding the main crack. Further imaging demonstrated the significance of the bone microstructure, such as the vasculature and osteocytes, in the distribution of the microdamage.*

INTRODUCTION

Bone is a unique material with a complex hierarchical structure that has the inherent ability to resist fracture [1-3]. The accurate and reliable prediction of fracture risk, and thus fracture prevention, in clinical situations therefore requires a detailed understanding of the crack propagation and fracture toughening mechanisms which occur at the different length scales. Several of the fracture toughening mechanisms that have been identified in bone include uncracked ligament bridging [2], crack branching and deflection [2], crack bridging by collagen fibrils [2], and energy dissipation via a microdamage process zone [3]. All of these mechanisms are significantly influenced by the bone structure and quality, in particular the material properties and the extent of pre-existing or accumulated microdamage.

At the ultrastructural level (nanoscale) bone is primarily a composite of the protein type-I collagen and the mineral hydroxyapatite. These constituents may be highly organised in their structure, as in the case of lamellar bone, or take a more random

arrangement as found in woven bone. Human cortical bone is formed predominantly of lamellar bone, while in larger and more rapidly growing animals, such as bovine, cortical bone can contain both the lamellar and woven type structures. In lamellar bone, the collagen and mineral form collagen fibrils (Fig. 1a) that are bundled together as collagen fibres (Fig. 1b). These fibres are further organised at the sub-microstructural level as lamellae (Fig. 1c). For the shaft of a human long bone, the lamellae form concentric rings around the entire bone (Figs 1c and 1d). Lamellar bone can also be arranged as smaller tubes of concentric layers, known as osteons or Haversian systems (Fig. 1c). The cortical bone in larger animals is usually comprised of plexiform type bone, which has a brick like structure of lamellar and woven bone. In addition to this complex structural hierarchy, throughout bone there is an extensive osteocyte-canalicular network as well as the vascular system. Osteocytes are tissue-resident bone cells, formed when the bone producing cells, osteoblasts, become trapped in the bone matrix. The osteocyte-canalicular network is thought to play a role in the detection of microdamage [4]. The composition and structure of bone can also vary greatly with such factors as skeletal site, age, sex, and the experienced mechanical loading [1].

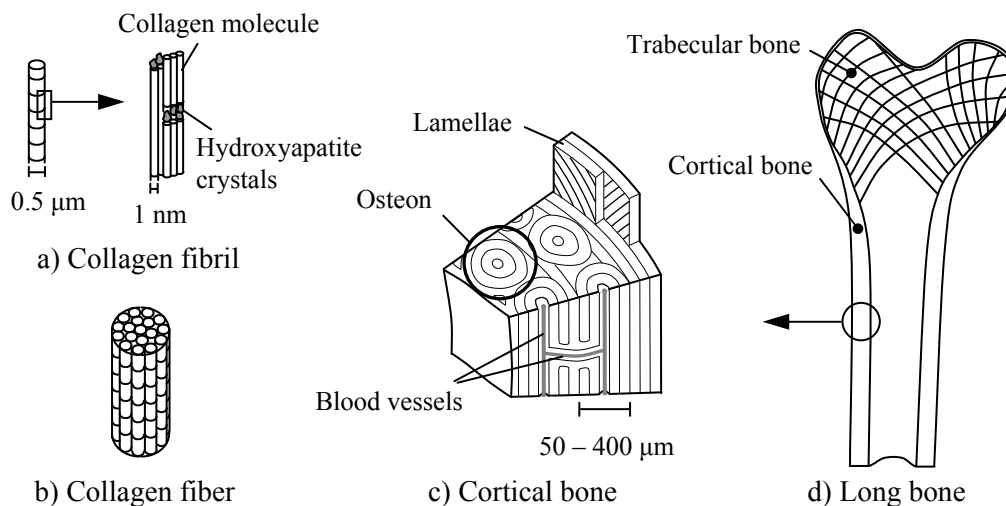


Figure 1. Hierarchical structure of human cortical bone (adapted from Rho et al. [1]).

Everyday cyclic loading of the skeletal structure, leads to the development of microdamage. This microdamage may take the form of ‘linear-type’ microcracks or more diffuse type matrix damage [3,5]. The development of fatigue microdamage is widely thought to be the stimulus for bone repair via targeted remodelling by the bone resorbing and bone forming cells osteoclasts and osteoblasts, respectively [4]. If the rate of damage accumulation exceeds that of the rate of repair, then stress fractures can occur [6]. This type of fracture is common in soldiers and athletes who undertake high intensity and repetitive activities, such as training exercises. Alternatively, if the rate of damage accumulation is considered to be normal, but the capacity for bone repair is reduced, due to aging or skeletal disease [7], fragility fractures can occur. Microdamage is also formed during ‘macrocrack’ propagation due to the high stress gradients at the

crack tip [2,3]. This damage contributes significantly to the fracture toughening mechanisms noted above and in some cases is the main source of the mechanism.

There have been numerous studies conducted into the formation and accumulation of microdamage in both trabecular and cortical bone [3,5,8,9]. Samples of bone tissue are first stained in order to label the microdamage either produced *in vivo* or through *in vitro* mechanical testing. Microdamage is then identified using techniques such as light microscopy, fluorescence microscopy, and more recently laser scanning confocal microscopy [3,5,8,9]. These studies have provided much insight into the formation of microdamage in relation to the microstructure and, to some extent, the applied loading.

The propagation of microcracks and larger ‘macrocracks’ in cortical bone has been investigated by exploiting the techniques of fracture mechanics [2]. Specially designed fracture and fatigue specimens are machined and a crack propagated from a starter notch. The crack length and load-displacement curve are monitored throughout the tests and used to determine the fracture toughness, fracture resistance or fatigue properties of the bone material. From these studies the crack morphology and interaction with the bone microstructure can be observed. A variety of fracture toughening mechanisms have been identified such as crack bridging and crack deflection, as noted previously.

The purpose of this paper is to present a novel technique for the investigation of crack propagation and microdamage in cortical bone using laser scanning confocal microscopy and sequential labelling with chelating fluorochromes [8]. The use of sequential labelling allows for tracking of the crack growth and microdamage formation through the bone matrix. Furthermore, laser scanning confocal microscopy can provide high resolution images of the three-dimensional structure, which will facilitate a new understanding into the nature of the crack propagation and microdamage formation.

MATERIAL AND SAMPLE PREPARATION

Compact tension fracture specimens were machined from the diaphyses of six bovine tibiae in the circumferential-longitudinal orientation. All samples were wet machined using a milling machine with a 150 mm diameter tungsten carbide slitting saw. The thickness of the specimens was 5 mm with a total specimen width of 25 mm. A 10 mm long starter notch was machined into the specimens in the longitudinal direction using the milling machine with a 30 mm radius fly cutter with a 60° point. After machining, the specimens were individually wrapped in saline-soaked gauze and stored in airtight containers at -30°C. On the day of testing, the specimens were thawed in water and their surface polished using progressively finer grades of abrasive paper.

METHODS

Crack propagation

The initiation and propagation of the crack in each specimen was achieved using a specially designed wedge loaded crack-propagating tool (see Fig. 2). A small wedge

block was inserted into the mouth of the starter notch and gradually advanced using a screw mechanism. Throughout the tests the specimen was kept hydrated with water and the crack propagation was monitored using a dissecting microscope. The use of a wedge loading tool allowed for the crack to be easily incremented in several stages. First, the crack was initiated and grown to a length of at least 5 mm from the notch tip. The sample was then removed from the crack-propagating tool for staining and imaging using laser scanning confocal microscopy. This is further detailed in the following section. After the first stage of imaging the specimen was returned to the crack-propagating tool and the crack further advanced another 5 to 9 mm.

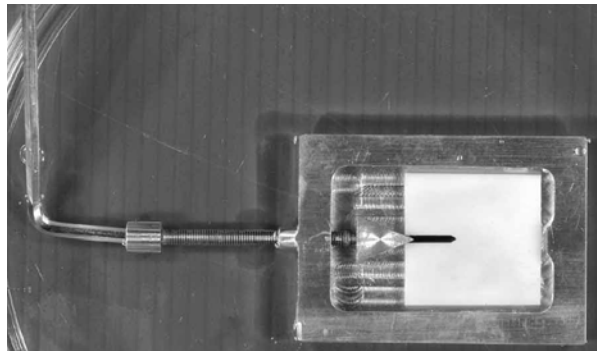


Figure 2. Compact tension specimen in wedge loaded crack-propagating tool [8].

Laser Scanning Confocal Microscopy and Fluorochrome Labelling

Laser scanning confocal microscopy was performed at five stages during the fracture tests. A Bio-Rad MRC-1000 imaging system was used, which was attached to an inverted Nikon Diaphot 300 microscope together with a Krypton/Argon laser. Images were obtained using $\times 4$ and $\times 40$ objective lenses at 20 μm below the surface as a z-series of images with a z-step of 5 μm ($\times 4$ objective) and 0.5 μm ($\times 40$ objective). Two chelating fluorochrome stains were utilised in this study to allow tracking of the main crack growth and microdamage progression. The chosen stains were xylenol orange and calcein. For xylenol orange a laser excitation of 568/10 nm and emission at 605/32 nm were used while for calcein the excitation was 488/10 nm and emission at 522/32 nm. In order to minimise fluorescence saturation and photo-bleaching, laser irradiation levels of 10 and 3 % were used for the xylenol orange and calcein, respectively.

The sequence employed for the imaging and labelling of the fracture specimens involved a series of five stages prior to, during and post-crack propagation. In this first stage (1), initial control images were made before the mechanical tests to identify any autofluorescence or other features of interest along the line of the crack. Following this, the crack was initiated and (2) further control images were made to examine the crack path and again check for autofluorescence. The specimens were then stained with xylenol orange (3) and re-imaged to observe the effects of the xylenol orange labelling. The fourth stage (4) of imaging was undertaken after the final crack propagation and served a similar purpose as stage (2). That is, the new crack path was examined and noted for any autofluorescence and to see if any of the xylenol orange from the previous

staining had penetrated into the extended crack. The test specimen was next stained with calcein (5) and imaged to observe the final crack morphology.

The fluorochrome labelling sequence was chosen based on the results from scratch tests. In these tests beams of cortical bone from the bovine tibiae were ‘scratched’ and labelled using two sequences, namely xylenol orange followed by calcein and calcein followed by xylenol orange. The sequence of xylenol orange and then calcein staining provided differential labelling of the surface scratches with the least dye substitution. For both the scratch tests and main fracture tests, the specimens were stained by immersion in a 5×10^{-4} M aqueous solution of the chosen stain and placed under vacuum for 24 h. The specimens were then rinsed under running water for 10 min ready for imaging.

RESULTS AND DISCUSSION

The initial confocal microscopy control images of the unstained specimens, showed no evidence of autofluorescence at the crack surface or at specimen depths of up to 200 μm . These observations were made using the settings for the xylenol orange and the calcein and for both lens objectives. Figure 3a displays a typical image for the xylenol orange stained initial crack length using the $\times 4$ objective. It was found that the fluorochrome was localised to the crack surfaces and stained to a visible depth of up to 200 μm . In Fig. 3b the calcein labelled extended crack as well as the initial xylenol orange crack are shown, again for the $\times 4$ objective. The calcein fluorochrome was primarily localised to the surfaces of the extended crack with minimal staining along the initial crack length. Furthermore, migration of xylenol orange into the extended crack was not observed for any of the specimens. Some regions of the bone vasculature had stained with both xylenol orange and calcein as can be noted from Figs 3a and 3b.

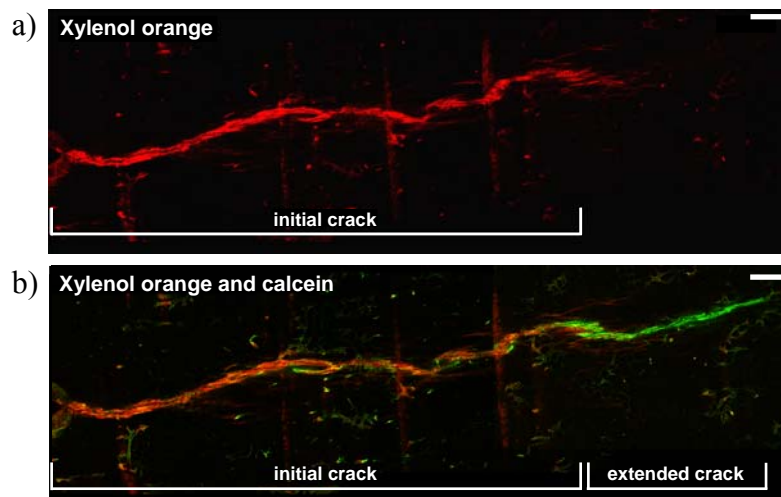


Figure 3. Laser scanning confocal microscopy images of a) the xylenol orange labelled initial crack, and b) the calcein labelled extended crack (bar = 500 μm) [8].

Higher objective imaging of the crack was simultaneously undertaken using the $\times 40$ objective lens. Figure 4 presents a higher objective image of the tip of an initial crack stained with xylenol orange, prior to any further crack extension. This image clearly demonstrates that there is a microdamage process zone (pz) surrounding the crack tip (ct). Within the process zone, there are numerous microcracks (mc) in the order of 20-100 μm in length and predominantly orientated in the longitudinal direction of crack growth. As the main crack (c) continues to propagate, this damage is left behind as a process zone wake (pzw) along the crack length. Vashishth et al. [3] have suggested that the formation of a microdamage process zone acts to slow down a propagating crack by dissipating fracture energy. Microcracks have also been implicated in a variety of extrinsic fracture toughening mechanisms such as crack deflection, branching and the formation of uncracked ligaments (see for example Ritchie et al. [2]).

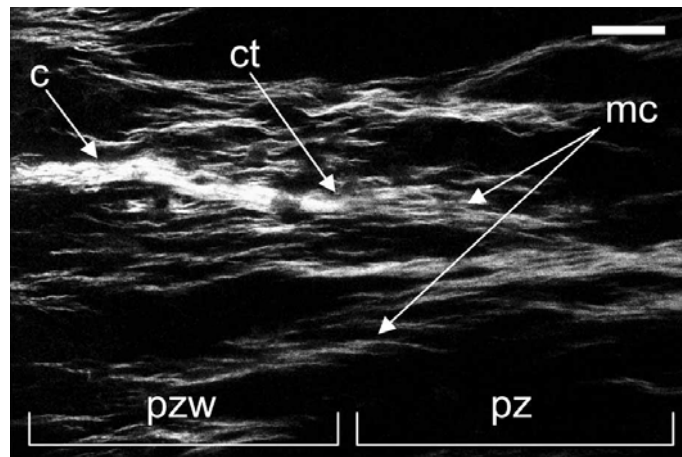


Figure 4. High objective ($\times 40$) confocal image of the tip of an initial xylenol orange stained crack prior to further crack extension (bar = 50 μm) [8].

The high resolution confocal imaging permits the investigation of the crack morphology and the interaction with bone microstructure. In particular, in certain regions surrounding the main crack, vascular canals (vc), and osteocyte lacunae and canaliculi (oc) were made visible with the calcein staining (Figure 5). These features appear to influence the sites of the microcracks (mc) by providing stress concentration and possible weak interfaces. A close up of the boxed region in Fig. 5 is shown in a z-series of images in Fig. 6 from 11 μm to 15.5 μm depth into the specimen. By compiling the series of images using three-dimensional (3D) reconstruction software (AmiraTM 3.0) it is possible to make a 3D image of the microcracks. Figure 7 displays a 3D reconstruction of the region in Fig. 5 for a total specimen depth of 25 μm . As in the Figs 5 and 6, this image is of a calcein stained region adjacent to the main crack. The 3D reconstructions show areas of diffusely stained microdamage (md), which suggests the involvement of submicroscopic tissue damage that is smaller than the resolution of the confocal microscope.

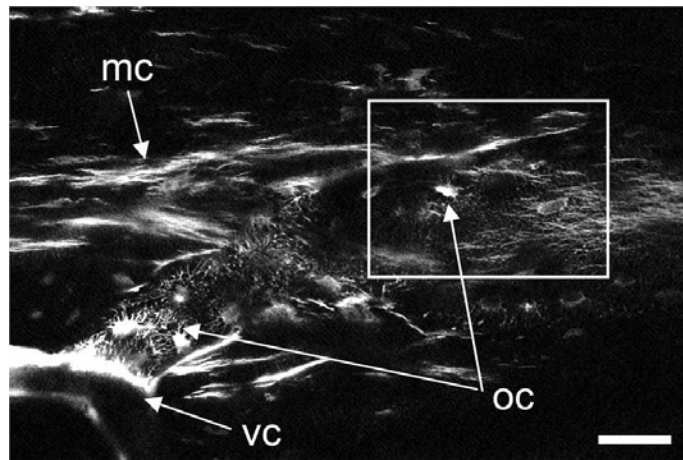


Figure 5. Confocal image of a calcein stained region adjacent to the main crack (bar = 50 μm) [8].

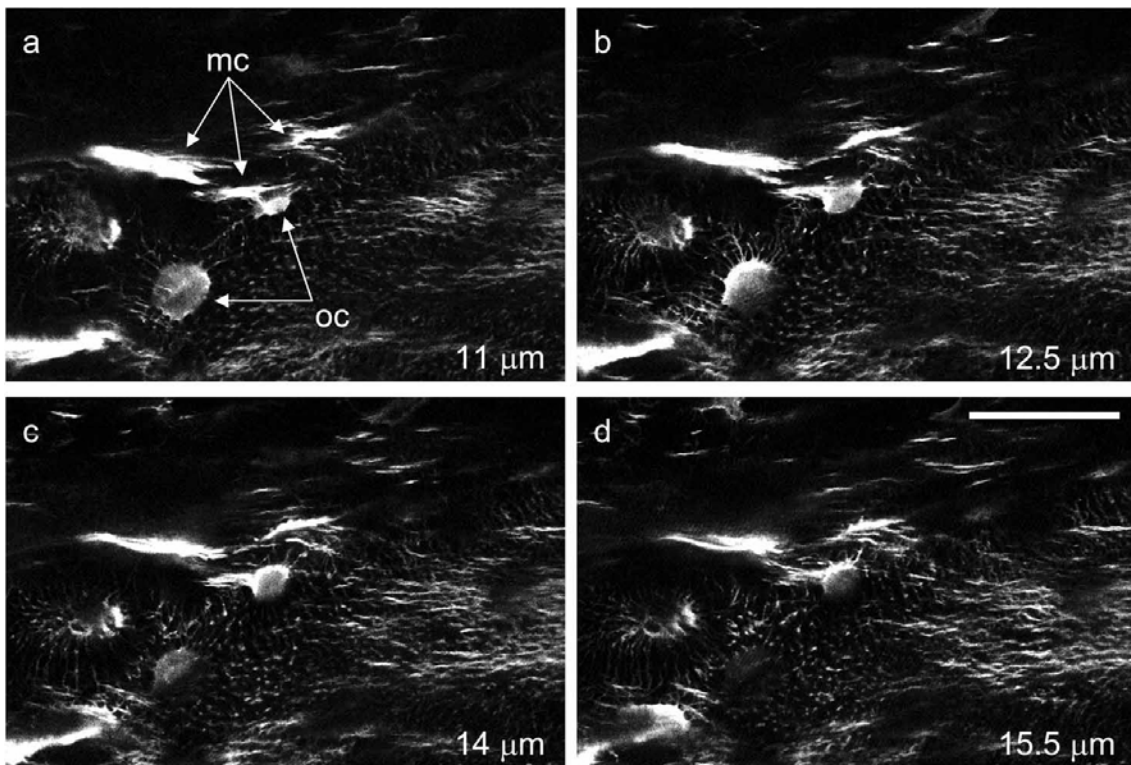


Figure 6. A z-series of confocal images of the boxed region in Fig. 5 for a calcein stained region adjacent to the main crack (bar = 50 μm) [8].

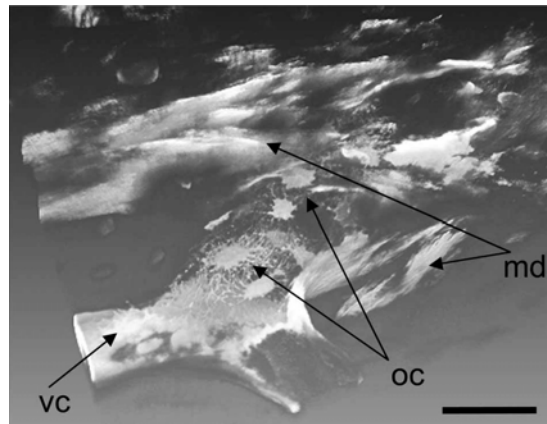


Figure 7. A three-dimensional reconstruction of the calcein stained region adjacent to the main crack and shown in Figs 5 and 6 (bar = 50 μm) [8].

CONCLUSION

Compact tension specimens were machined from the cortical bone of bovine tibiae and fracture tested in a wedge loaded crack-propagating tool. A two stage staining process was employed with xylenol orange and calcein being used to label the initial and extended cracks, respectively. Laser scanning confocal microscopy was utilised to produce two and three-dimensional images of the crack and surrounding regions. In all cases, the microdamage formation was influenced by the bone microstructure, including the presence of osteocytes and the vasculature. The techniques presented in this study can provide for a new understanding into crack propagation and microdamage, and how it relates to the bone material properties, structure and fracture resistance.

REFERENCES

1. Rho, J.Y., Kuhn-Spearing, L., Zioupos, P. (1998) *Med. Engng. Phys.* **20**, 92-102.
2. Ritchie, R.O., Kinney, J.H., Kruzic, J.J., Nalla, R.K. (2005) *Fatigue Fract. Engng. Mater. Struct.* **28**, 345-371.
3. Vashishth, D. (2007) *Int. J. Fat.* **29**, 1024-1033.
4. Burr, D.B. (2002) *Bone* **30**, 2-4.
5. Lee, T.C., Mohsin, S., Taylor, D., Parkesh, R., Gunnlaugsson, T., O'Brien, F.J., Giehl, M., Gowin, W. (2003) *J. Anat.* **203**, 161-172.
6. Burr, D.B. (1997) *Exerc. Sport Sci. Rev.* **25**, 171-194.
7. Zioupos, P. (2001) *J. Microsc.* **201**, 270-278.
8. Zarrinkalam, K.H., Kuliwaba, J.S., Martin, R.B., Wallwork, M.A.B., Fazzalari, N.L. (2005) *Eur. J. Morphol.* **42**, 81-90.
9. Fazzalari, N.L., Forwood, M.R., Manthey, B.A., Smith, K., Kolesik, P. (1998) *Bone* **23**, 373-378.